Integrative single-cell analysis reveals endothelial diversity in the vasa vasorum of human atherosclerosis

Author name and affiliations:

Yanzhao Wu[1, 2*], Zhiwei Xue[1, 2*], Tao Sun[1, 2*], Yinda Yu[3], Xiangjun Liang[1, 2], Wenchen Xing[1, 2], Feiyu Mu[1, 2], Zhihan Zhang[1, 2], Meilin Lv[1, 2], Lu Ling[1, 2], Mengtao Han[1, 2], Lian Cheng[1, 2#], Anton Gisterå[3#], Donghai Wang[1, 2, 4#]

1. Department of Neurosurgery, Qilu Hospital, Cheeloo College of Medicine and Institute of Brain and Brain-Inspired Science, Shandong University, Jinan, China.

2. Shandong Key Laboratory of Brain Health and Function Remodeling, Jinan, China.

3. Department of Medicine Solna, Center for Molecular Medicine, Karolinska University Hospital, Karolinska Institutet, Stockholm, Sweden.

4. Department of Neurosurgery, Qilu Hospital of Shandong University Dezhou Hospital, Dezhou, China.

* These authors contributed equally.

#Corresponding Authors:

Donghai Wang, Ph.D. and M.D. (drwangdonghai@sdu.edu.cn); Anton Gisterå, Ph.D. and M.D. (anton.gistera@ki.se); Lian Cheng, Ph.D. and M.D. (chenglian5667@163.com)

This supplementary information contains:

- Supplementary Tables (3 Tables, 1 to 3)
- Supplementary Figures (8 Figures, 1 to 8)

Supplementary Table 1: Patient metadata

Dataset	Tissue	Sex	Age	GEO Accession or link
Alsaigh 1	Carotid	Male	82	GSM4837523, GSM4837524
Alsaigh 2	Carotid	Male	87	GSM4837525, GSM4837526
Alsaigh 3	Carotid	Male	65	GSM4837527, GSM4837528
Wirka 1	Coronary	Male	65	GSM3819856, GSM3819857
Wirka 2	Coronary	Male	54	GSM3819858, GSM3819859
Wirka 3	Coronary	Male	65	GSM3819860, GSM3819861, GSM3819862
Wirka 4	Coronary	Female	58	GSM3819863
Hu 1	Coronary and aortic	Male	54	https://zenodo.org/record/6032099#.Y1RDa-zMITU
Hu 2	Coronary and aortic	Male	44	https://zenodo.org/record/6032099#.Y1RDa-zMITU
Hu 3	Coronary and aortic	Female	46	https://zenodo.org/record/6032099#.Y1RDa-zMITU
Bashore 4	Carotid	Male	89	GSM8029962
Bashore 6	Carotid	Male	67	GSM8029963
Bashore 9	Carotid	Male	64	GSM8029964
Bashore 13	Carotid	Female	66	GSM8029965
Bashore 14	Carotid	Male	46	GSM8029966
Bashore 15	Carotid	Female	76	GSM8029967
Bashore 16	Carotid	Male	62	GSM8029968
Bashore 17	Carotid	Male	64	GSM8029969
Bashore 18	Carotid	Male	66	GSM8029970
Bashore 19	Carotid	Male	75	GSM8029971
Bashore 20	Carotid	Male	58	GSM8029972
Bashore 21	Carotid	Male	59	GSM8029973
Pan 1	Carotid	Male	83	GSM4705589
Pan 2	Carotid	Male	67	GSM4705590
Pan 3	Carotid	Female	76	GSM4705591

Supplementary Table 2: Carotid atherosclerotic plaque patients

Patient	Gender	Age at Surgery
Patient 1	Female	58
Patient 2	Female	74
Patient 3	Male	60
Patient 4	Male	74

Supplementary Table 3: Antibodies used in this study

Antibodies	Manufacturer	Cat No.	Applications
SULF1	Proteintech	27438-1-AP	IF, 1:100
ACKR1	Proteintech	55185-1-AP	IF, 1:100
NR2F2	ABclonal	A10251	IF, 1:100
PECAM1	Servicebio	GB12064-100	IF, 1:100
CD144	Proteintech	APC-FcA98071	FACS, 1:20

Supplementary Figure 1

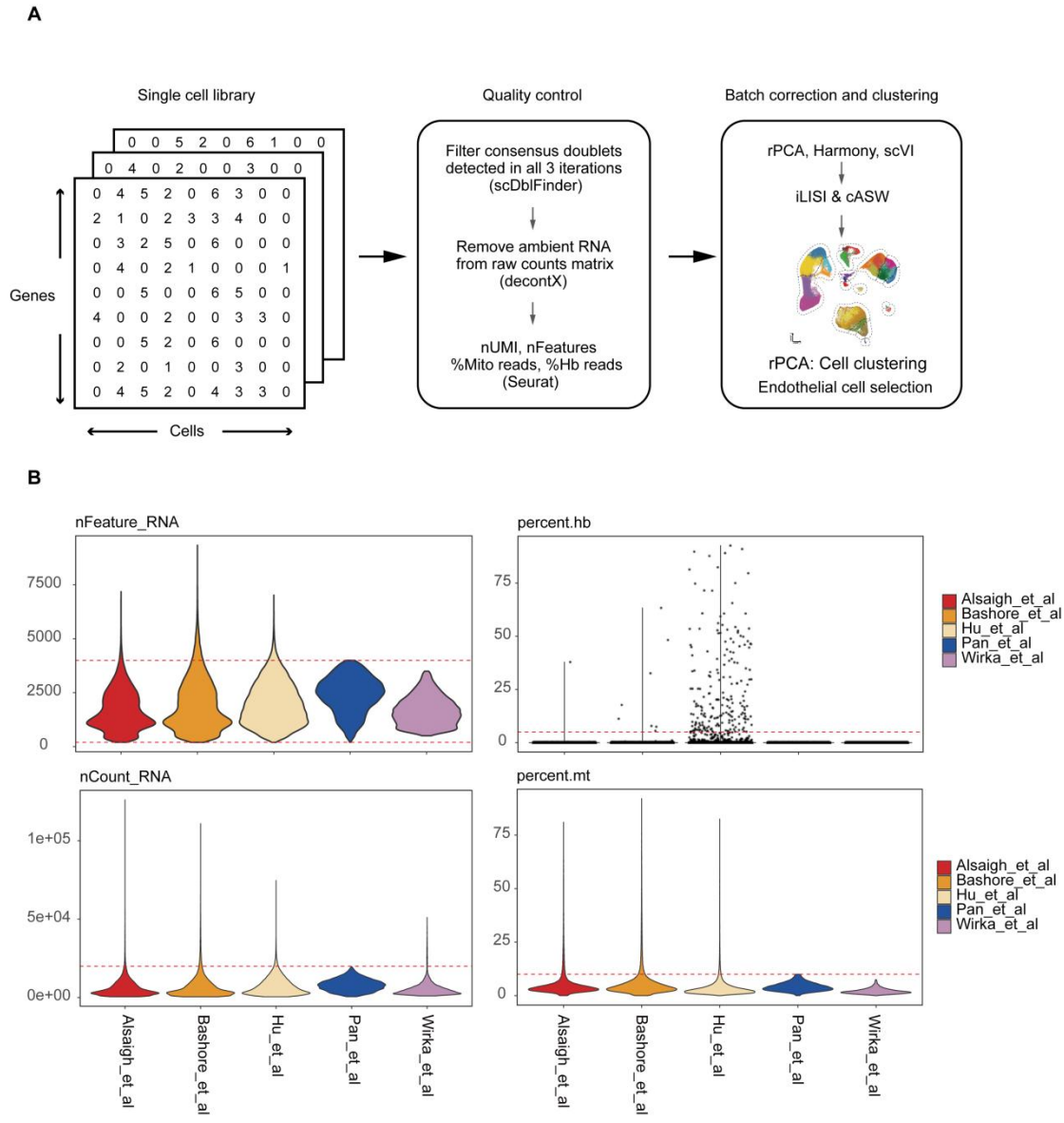

Supplementary Figure 1: Single-cell RNA-seq quality control and integration workflow.

A Schematic of the analysis pipeline. Raw gene-by-cell count matrices were processed by (i) filtering consensus doublets detected across three iterations of scDblFinder; (ii) removing ambient RNA with decontX; and (iii) per-cell QC using Seurat metrics (nUMI, nFeature, % mitochondrial reads, % hemoglobin reads). Datasets were then integrated using rPCA, Harmony, and scVI, with batch correction assessed by iLISI and cASW. **B** QC distributions across five public datasets. Violin plots showed nFeature_RNA and nCount_RNA, and the percentages of hemoglobin (percent.hb) and mitochondrial (percent.mt) reads. Dashed red lines indicated filtering cutoffs; points depict individual cells.

Supplementary Figure 2

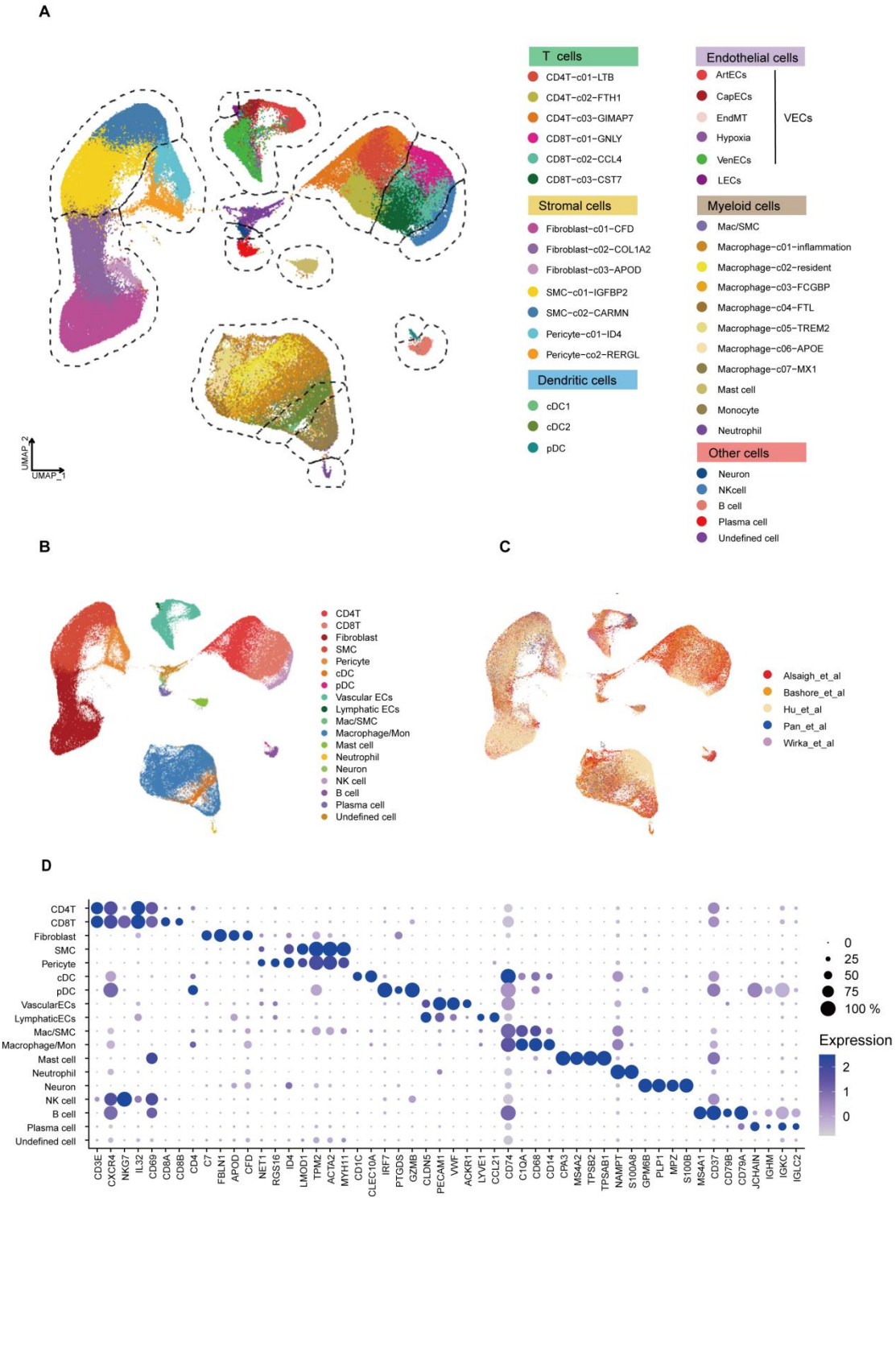

Supplementary Figure 2: Landscape of atherosclerosis at single-cell resolution.

(**A, B**) UMAP plots of 200,430 cells based on rPCA integration of 38 sequencing samples. **C** UMAP plots for tested integration approaches. **D** Dot plots illustrating the expression patterns of corresponding signature genes for each cluster.

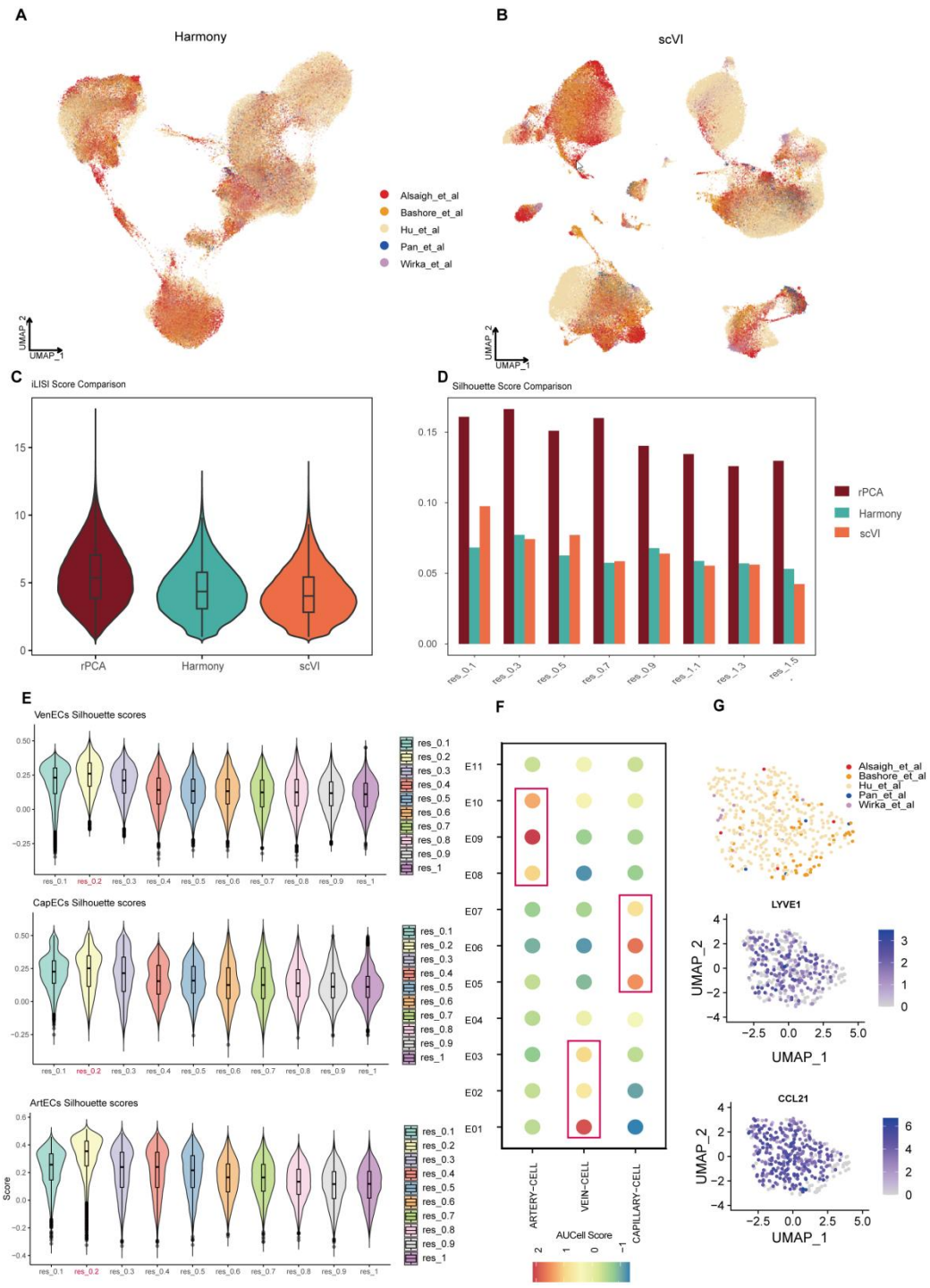
A
Harmony
Alsaigh_et_al
Bashore_et_al
Hu_et_al
Pan_et_al
Wirka_et_al
UMAP_2
UMAP_1
B
scVI
UMAP_2
UMAP_1
C
iLISI Score Comparison
rPCA
Harmony
scVI
D
Silhouette Score Comparison
rPCA
Harmony
scVI
E
VenECs Silhouette scores
CapECs Silhouette scores
ArtECs Silhouette scores
Score
F
ARTERY~CELL
VEIN~CELL
CAPILLARY~CELL
AUCell Score
G
Alsaigh_et_al
Bashore_et_al
Hu_et_al
Pan_et_al
Wirka_et_al
LYVE1
CCL21
UMAP_2
UMAP_1

Supplementary Figure 3: Benchmarking integration strategies and annotating endothelial subclusters.

(**A, B**) UMAP plots for integration approaches tested using Harmony or scVI. **C** Violin plots showing the distribution of iLISI values after each integration approach. Each violin illustrated the kernel density of the data. The center line represented the median, and the width of the violin reflected the data distribution across values. **D** Mean cASW coefficients calculated for each integration approach. **E** Mean cASW coefficients calculated for different endothelial subclusters. The final selected resolution was indicated in red. **F** Dot plots illustrating AUCell-based cell type scores across subclusters. **G** Integration of lymphatic endothelial cells using rPCA, along with visualization of marker gene expression.

Supplementary Figure 4

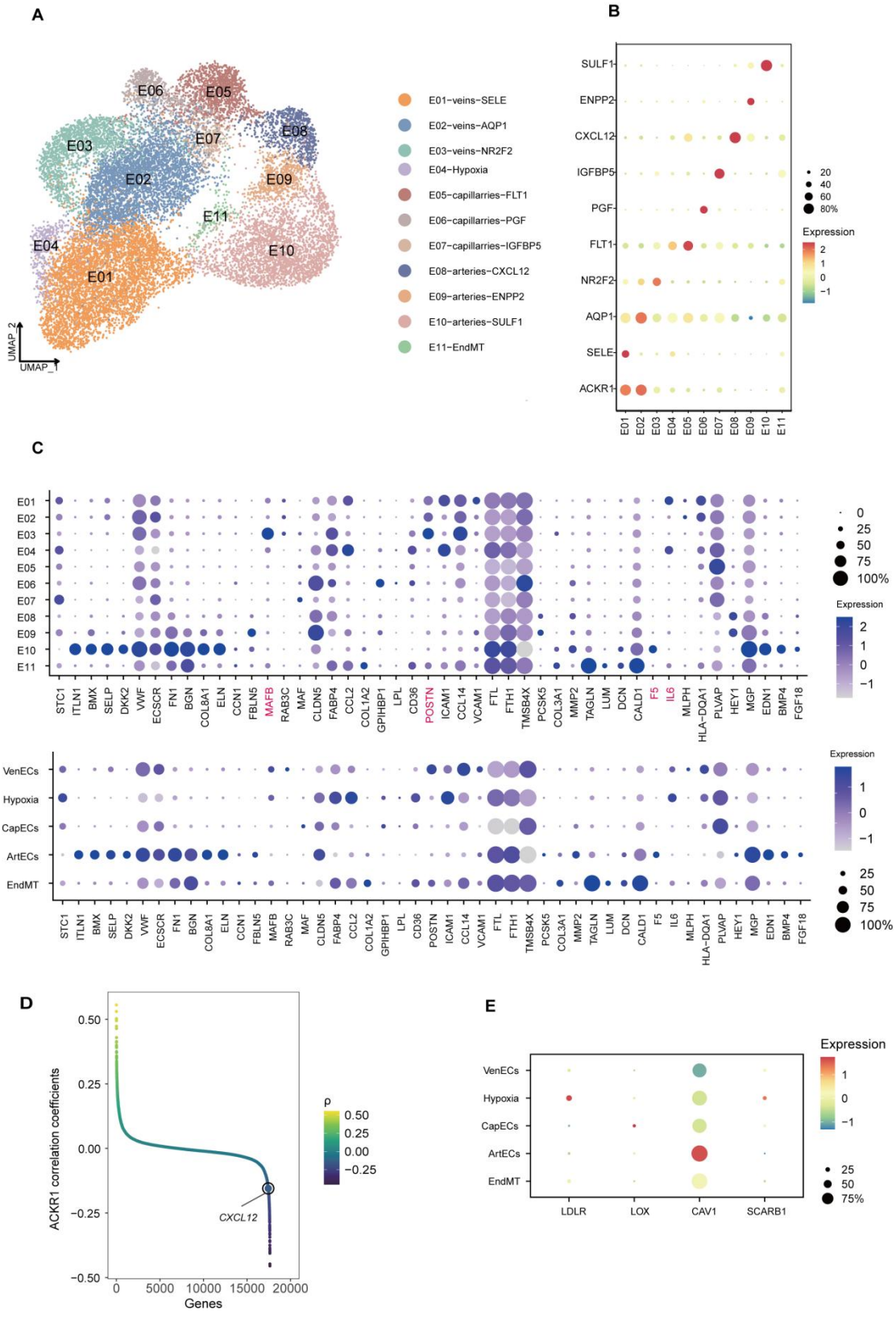

Supplementary Figure 4: Definition and characterization of vascular endothelial cells based on single-cell transcriptomic data.

A UMAP plots of 17,367 vascular endothelial cells based on rPCA. **B** Dot plots illustrating the expression patterns of corresponding signature genes for each subcluster. **C** Dot plots illustrating the expression patterns of previously used signature genes. **D** Spearman correlation plot of *ACKR1* versus all genes across VECs. Spearman correlation coefficients (ρ) were represented by color. **E** Dot plots illustrating the expression patterns of genes related to LDL uptake by endothelial cells.

Supplementary Figure 5

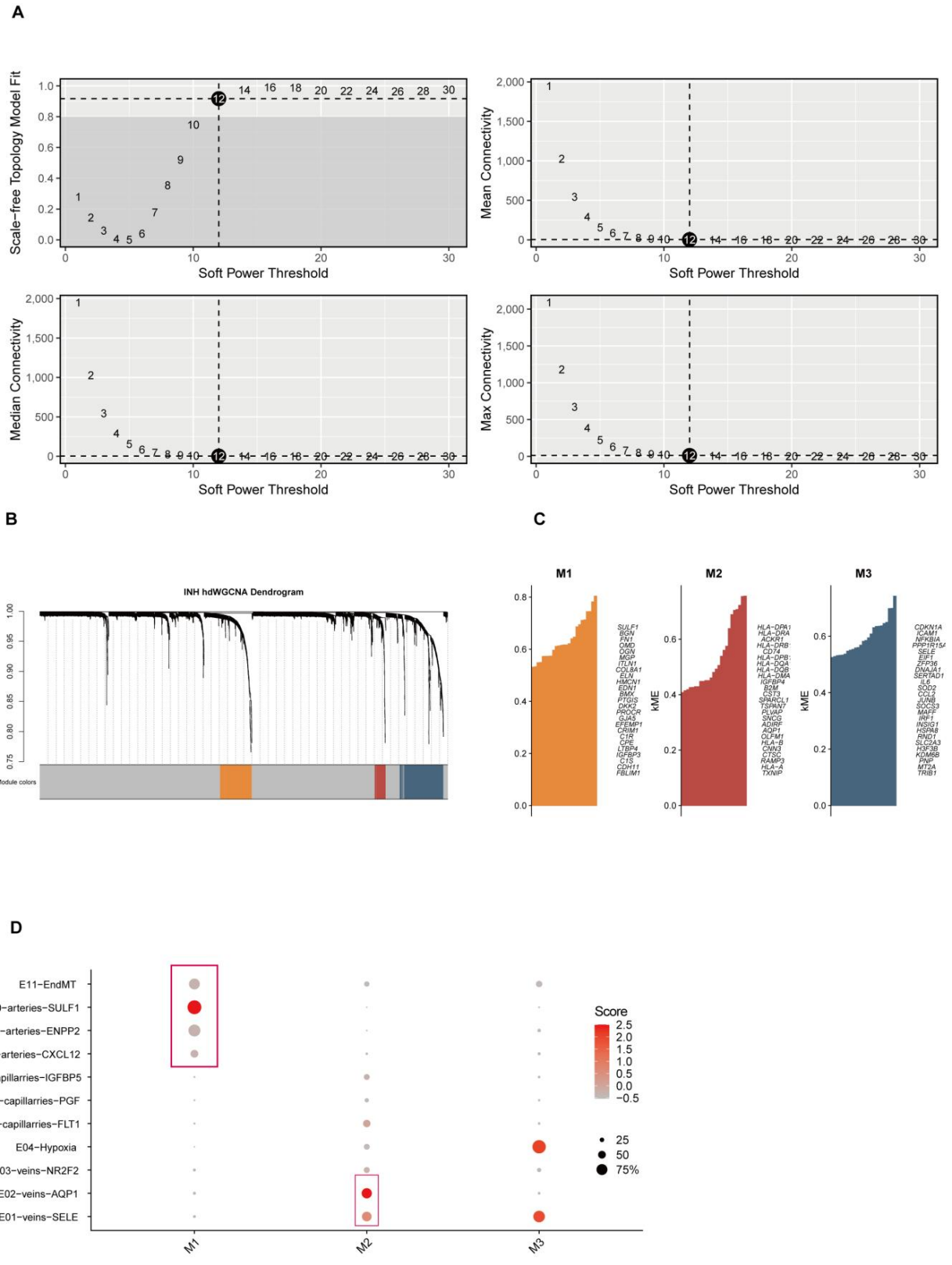

Supplementary Figure 5: hdWGCNA co-expression modules in vascular endothelial cells.

A Selection of the soft-thresholding power for hdWGCNA network construction. **B** hdWGCNA dendrogram showing the identified co-expression modules. **C** The top 25 genes in each module ranked by eigengene-based connectivity. **D** Dot plots of module eigengene (ME) scores across subclusters. The size of the dot indicated the proportion of cells expressing the ME scores greater than 0, while the color intensity reflected the average ME score level across subclusters.

Supplementary Figure 6

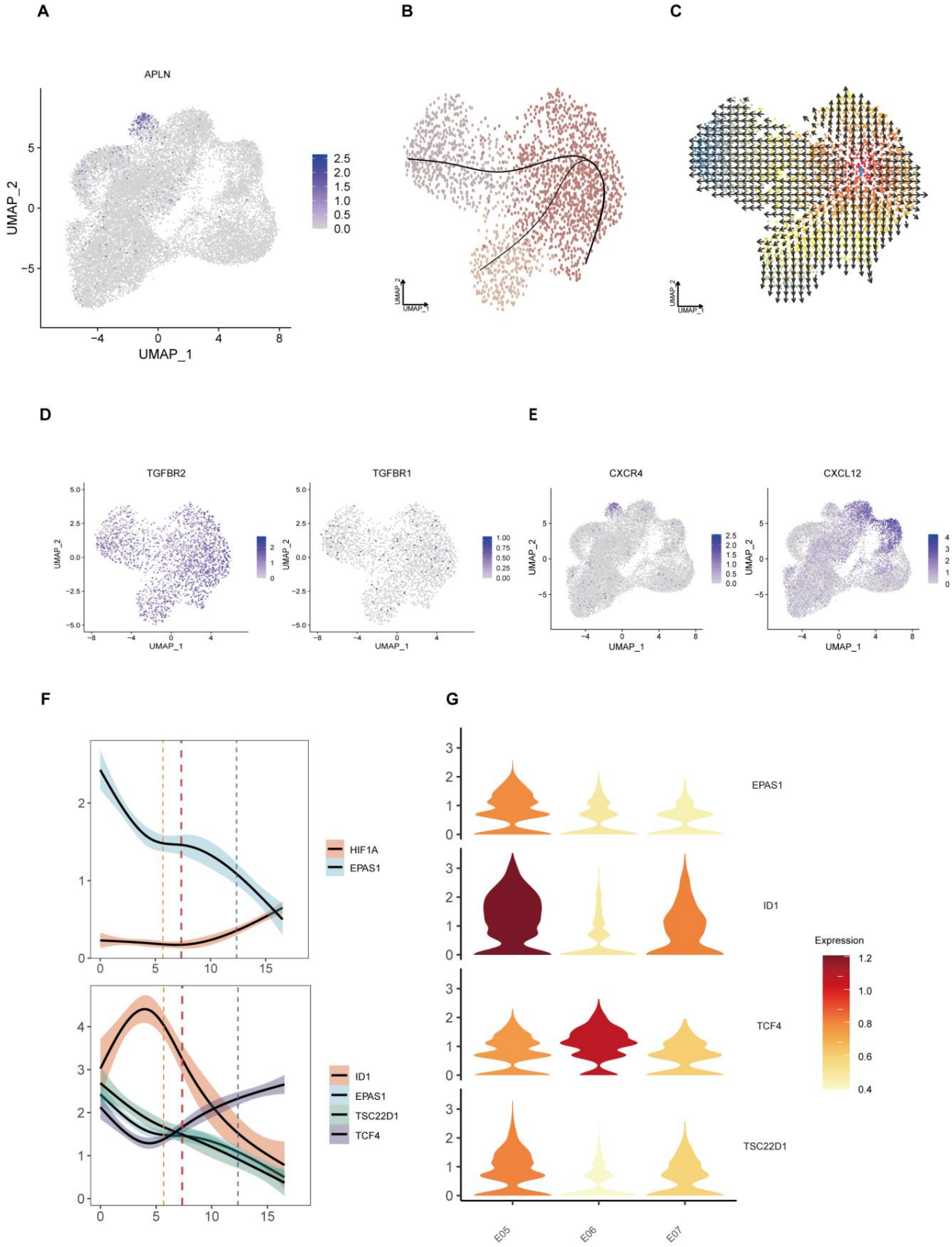

Supplementary Figure 6: Angiogenesis in atherosclerotic plaques.

A Featureplots showing the expression of *APLN*. **B** UMAP plots showing the pseudotime trajectory calculated with Slingshot in CapECs. **C** The vector representation of developmental directions for cells in CapECs using VECTOR. The pseudotime order of cells was shown by color (from red to blue). **D** Featureplots showing the expression of *TGFBR2* and *TGFBR1* in CapECs. **E** Featureplots showing the expression of *CXCR4* and *CXCL12*. **F** Cubic spline interpolation of gene expression across pseudotime with 95% confidence intervals. **G** Violin plots showing gene expression patterns.

Supplementary Figure 7

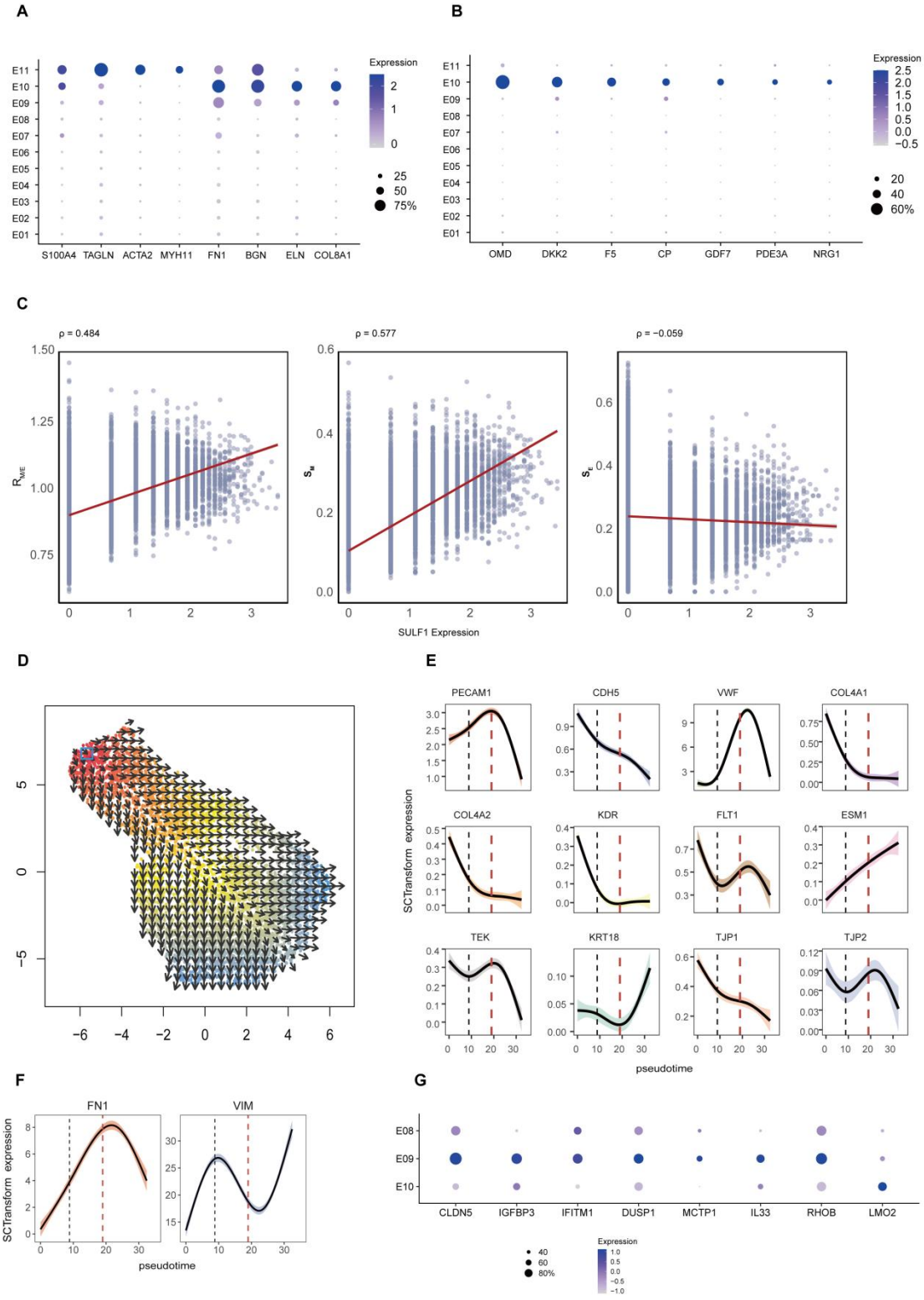

Supplementary Figure 7: Endothelial-to-mesenchymal transition.

(**A, B**) Dot plots illustrating the gene expression. **C** Spearman correlation between *SULF1* expression and $R_{M/E,}$ S_M and S_E. Spearman correlation coefficient (ρ) was used to assess the association. **D** The vector representation of developmental directions for cells in ArtECs using VECTOR. **E** Cubic spline interpolation of gene expression across pseudotime with 95% confidence intervals. **F** Cubic spline interpolation of *FN1* and *VIM* expression across pseudotime with 95% confidence intervals. **G** Dot plots illustrating the transcription factor expression.

Supplementary Figure 8

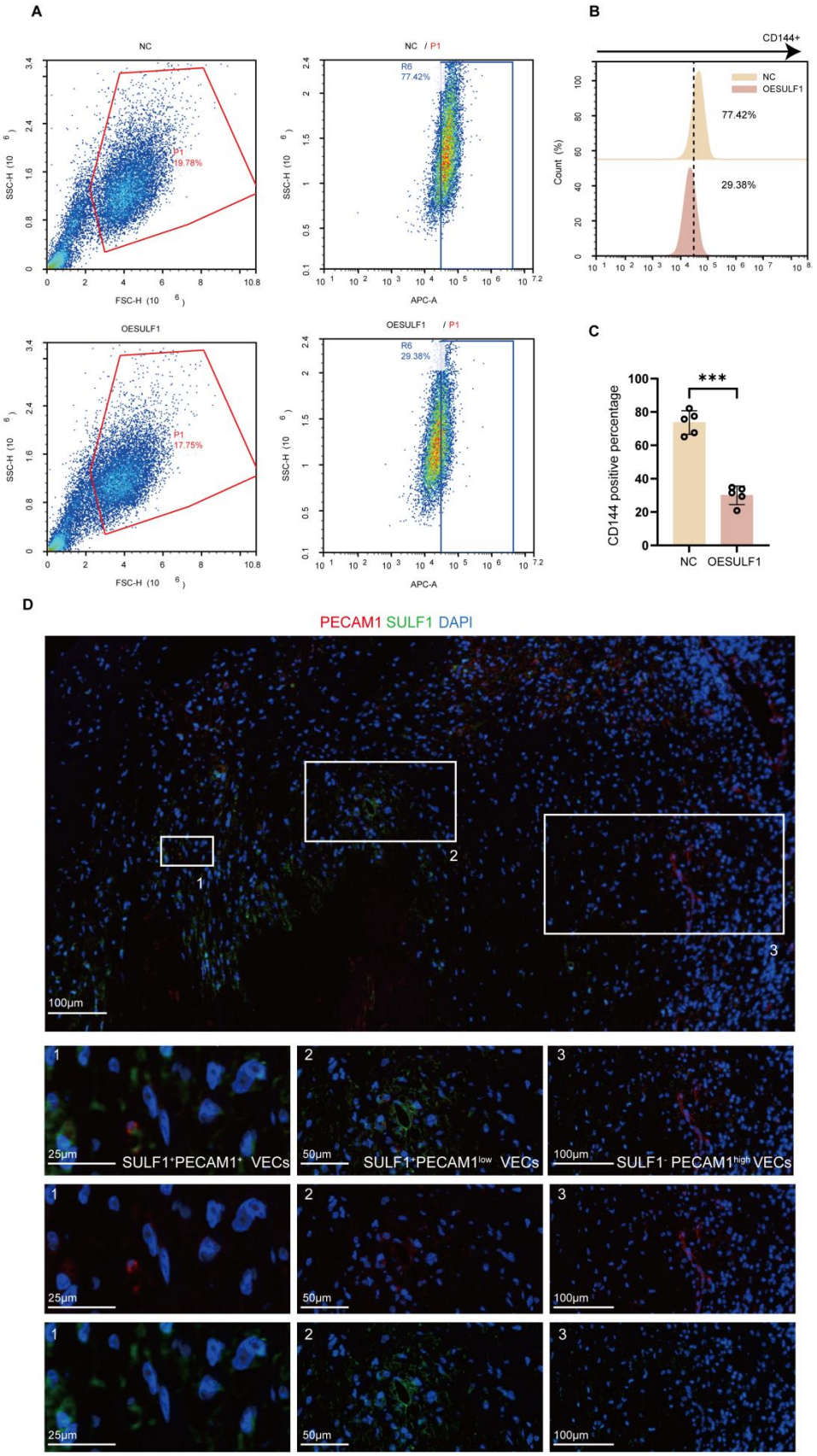

Supplementary Figure 8: SULF1 reduced endothelial CD144 (VE-cadherin) expression; immunofluorescence co-staining of SULF1 and PECAM1.

A Representative flow-cytometry plots showing the gating strategy for analysis of surface CD144 (VE-cadherin) in HUVECs 48 h after transfection with NC (negative control) or OESULF1 (SULF1 overexpression). **B** Flow-cytometry histograms of surface CD144 (VE-cadherin) in HUVECs 48 h after transfection (NC vs OESULF1). Dashed line indicated the $CD144^+$ gate; numbers denoted the percentage of $CD144^+$ cells. **C** Quantification of $CD144^+$ percentage (mean ± SEM; n = 5 per group). Statistics: unpaired Welch's t test, $^{***}p < 0.001$. **D** Representative immunofluorescence images of human carotid endarterectomy plaque from Qilu Hospital (patient 1; see Supplementary Table 2) showing co-staining for PECAM1 and SULF1. Nuclei were counterstained with DAPI. Scale bars: 100 μm in the overview image; 25 μm (1), 50 μm (2) and 100μm (3).